RSC Sustainability

ROYAL SOCIETY OF CHEMISTRY

COMMUNICATION

View Article Online
View Journal | View Issue

Cite this: *RSC Sustainability*, 2026, **4**, 228

Received 8th September 2025
Accepted 24th November 2025

DOI: 10.1039/d5su00734h

rsc.li/rscsus

Polypropylene microplastic degradation using ultraporous polarized hydroxyapatite and sunlight

Marc Arnau, †[ab] Jordi Sans†*[abc] and Carlos Alemán *[abc]

The development of effective technologies to remove microplastics (MPs) from both aquatic and terrestrial environments is an urgent necessity. As a proof of concept, here we show the catalytic degradation of polypropylene MPs and their transformation into chemicals using a permanently polarized novel metal-free bioceramic catalyst and sunlight.

Sustainability spotlight

Globally, microplastic pollution has become a serious environmental threat due to their multiple sources, widespread occurrence, persistence, and adverse effects to the ecosystem and human health. Unfortunately, conventional recycling approaches for plastics are not suitable to reduce microplastic pollution. In this work, we use a bioceramic noble metal-free catalyst, which was previously employed to produce organic molecules using simple gases such as carbon dioxide and methane, to transform polypropylene microplastics into small alcohols, such as ethanol and isopropanol. The selectivity of the catalyst (up to 95%), which is photoactivated with solar light, is modulated through the presence of water in the reaction medium and power illumination.

Microplastics (MPs), which are plastic particles ranging in size from 0.1 to 5 mm,[1] are a serious environmental concern due to their prevalence in aquatic and terrestrial environments. Once released into the environment, MPs can persist for decades, and potentially centuries, due to their resistance to degradation.[2] Such long term durability and persistence, combined with their easy transportability, adversely affect not only the ecosystem but also the health of humans and animals, as concluded from different studies in living organisms.[3] Unfortunately, conventional recycling approaches for plastics are not suitable to reduce MP pollution.[4] For example, MPs removed by conventional wastewater treatment plants (with a rate higher than 90%[5]) are simply discharged into natural waterbodies or retained in the sludge.[6] Therefore, much research on specific technologies is still necessary to define efficient and environmental friendly approaches to eliminate MPs from the environment.

Different advanced technologies have been proposed for removing MPs from water, such as the physical adsorption,[7] photodegradation, photocatalytic degradation, photoreforming,[8] and biological processes.[9] Physical adsorption of MPs over adsorbents (*e.g.* zeolites) presents some disadvantages, for example, generation of contaminants, sludge removal along with MPs, high operational cost and a decreased removal rate.[7] Photodegradation and photocatalytic degradation enable depolymerisation and upcycling of MPs under mild conditions, but may produce toxic by-products and have a high cost, while photoreforming promotes selectivity by accurately scissoring the MP chemical bonds.[8] Finally, biological processes, in which degradation is induced by biological entities such as microbes and enzymes, have lower cost but frequently exhibit slow degradation rates and require genetic manipulation, which limit their scalability.

Ultraporous permanently polarized hydroxyapatite (upp-HAp) is an effective catalyst for the synthesis of small organic compounds, such as acetic acid, ethanol, ammonia and urea, starting from small molecules in the gas phase, like CO_2 or/and N_2.[10] During this construction process, which occurs under mild reaction conditions, chemical bonds are efficiently formed. In this study, we show the versatility of upp-HAp as a catalyst by revealing its ability to disrupt stable chemical bonds. This is an uncommon property since catalysts used for the synthesis of chemicals from small gas molecules rarely function in the depolymerization of stable polymers. Furthermore, we show that upp-HAp, which performs efficiently in the gas–solid heterogeneous catalytic process, is also effective in the solid–solid catalytic photodegradation of MPs into small organic

[a]*IMEM-BRT Group, Departament d'Enginyeria Química, EEBE, Universitat Politecnica de Catalunya - BarcelonaTech, C/ Eduard Maristany, 10-14, 08019, Barcelona, Spain. E-mail: Jordi.sans.mila@upc.edu; carlos.aleman@upc.edu*

[b]*Barcelona Research Center in Multiscale Science and Engineering, Universitat Politècnica de Catalunya - BarcelonaTech, 08930 Barcelona, Spain*

[c]*Institute for Bioengineering of Catalonia (IBEC), The Barcelona Institute of Science and Technology, Baldiri Reixac 10-12, 08028 Barcelona, Spain*

† These two authors contributed equally to this work.

molecules. For this purpose, polypropylene (PP; M_n = 50 000 and M_W = 190 000) was selected as the carbon source, sunlight as the energy source, and upp-HAp as the catalyst for plastic transformation and selective fabrication of small alcohols, such as ethanol (EtOH) and isopropanol (^{i}PrOH).

upp-HAp was prepared using a two step process (Fig. 1a).[11] The first step consisted of the calcination of synthesized hydroxyapatite (HAp) in air at 1000 °C to generate irreversible OH^- vacancies (thereby, to remove the steric hindrance in OH^- columns of HAp), while the thermally stimulated polarization (TSP) treatment was applied in the second step to impose a specific orientation to all remaining OH^- groups. The TSP consists of applying a high DC electric field at high temperature (125 V cm^{-1} at 1000 °C) to the previously calcined specimen (c-HAp). Details on the preparation process are provided in the SI.

The X-ray diffractogram and Raman spectrum of upp-HAp show not only the characteristic peaks of HAp but also those of brushite (Fig. S1), reflecting the structural changes induced by the TSP treatment.[12] The Nyquist plots collected for upp-HAp and calcined HAp (c-HAp) discs in the dry state and after adding 50 μL of a 3.5% NaCl solution on the samples to enhance ion transport (also mimicking the wet working conditions of the reactions) are compared in Fig. 2a and b, while Table S1 lists the values of the equivalent electrical circuit (EEC) elements used to fit the electrochemical impedance spectroscopy results (included in Fig. 2a and b). Measurements in the dry state indicate that the resistance of c-HAp (control) decreases by two orders of magnitude after the TSP treatment (from 568.7 MΩ cm^{-2} to 9.6 MΩ cm^{-2}). Although the TSP effect is less pronounced in the wet samples, the reduction is still significant (from 9.7 MΩ cm^{-2} to 1.6 MΩ cm^{-2}).

Scanning electron microscopy (SEM) images reflect the porosity of upp-HAp (Fig. 2c). The average pore size, as estimated from SEM micrographs, is 172 ± 56 nm while the average size of the coalesced nanoparticles is 159 ± 43 nm. This result is in agreement with the Brunner–Emmett–Teller (BET) surface area analysis, which provides a pore diameter and a total surface area of 144 ± 15 nm and 3.82 ± 0.05 m^2 g^{-1}, respectively. High-resolution transmission electron microscopy (HRTEM) images confirm the presence of highly crystalline HAp grains with well-defined lattice fringes (Fig. 2d). Moreover, the Fourier transform image allows the identification of well-resolved fringes at 2.8, 3.4 and 7.0 Å, which are attributed to the (211), (002) and (001) crystallographic planes of HAp (Fig. 2d, inset). Overall, the results displayed in Fig. 2a–c prove that upp-HAp fulfils the conditions to be considered as a catalytically active material.[11] The UV-vis absorption capacity of c-HAp and upp-HAp is compared in Fig. 2e. While c-HAp does not absorb light at any wavelength, the photoabsorption capacity of upp-HAp in the solar spectrum is indicated by the absorption peaks at 236 and 360 cm^{-1} (UVA and UVC regions). The complete absorption spectra are shown in Fig. S2. The band gap energies (B_g), which were determined using the approach developed by Makula *et al.*[13] for the Tauc method, confirmed the visible light activity (Fig. S3).

PP isotactic (M_w ~190 000) was purchased from Sigma Aldrich (427896-1KG). The manufacturer provided 3–4 mm diameter pellets which were thoroughly ground by means of cryo-ball milling employing a Retsch MM 400 working at 25 Hz for 5 min. Fig. S4 displays the size of the resulting particles (0.48

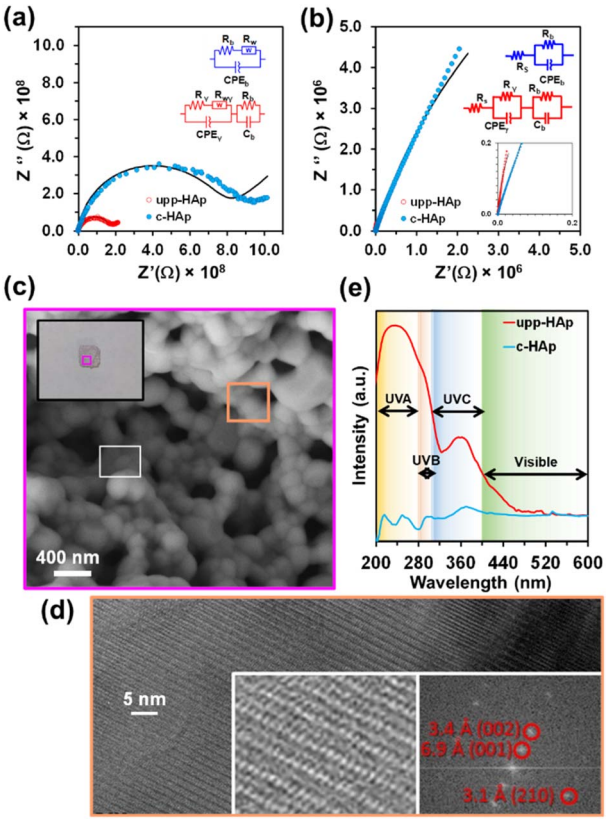

Fig. 2 (a and b) Nyquist plots of upp-HAp and c-HAp discs in the (a) dry and (b) wet state (*i.e.* adding 50 μL of a 3.5% NaCl solution). The EECs used to fit the experimental data are included as insets (Tables S1 and S2). (c) Digital photograph, and SEM and HRTEM images of upp-HAp. Fourier transform of the images is also displayed. (d) UV-vis absorption spectra of upp-HAp and (e) c-HAp.

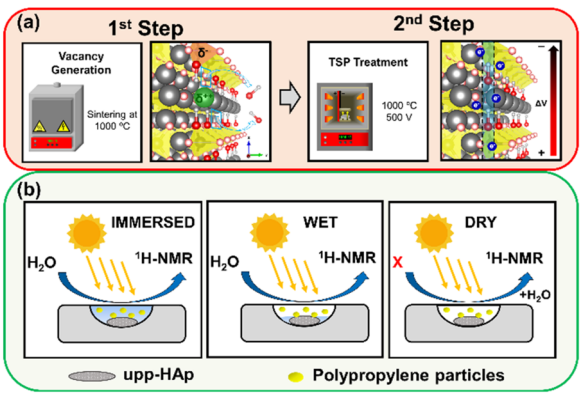

Fig. 1 (a) Steps used to prepare the upp-HAp catalyst, sketching the induced structural alterations. (b) Conditions used to transform polypropylene waste into chemical products: immersed in water (left), wet (middle) and dry (right) using upp-HAp catalysts and 1 sun solar irradiation.

± 0.21 mm on average) and representative optical and SEM micrographs. The effective conversion of PP plastic waste (30 mg) into chemicals, ^{i}PrOH and EtOH, using the upp-HAp catalyst (20 mg) and 1 sun solar irradiation (*i.e.* by convention, 1 sun is defined as 1000 W m^{-2} of solar irradiance, corresponding to standard illumination at AM1.5.) was investigated, which is sketched in Fig. 1b, considering: (1) the catalyst and the PP waste immersed in 200 μL of water; (2) the catalyst in a wet state (*i.e.* with water adsorbed at its surface only); and (3) the catalyst and the PP in a dry state (*i.e.* water vapour supplied from atmospheric humidity only). In all cases, samples were kept under such conditions for 2 h. After such a short time, ^{1}H NMR spectra were acquired considering the water introduced in the holder for immersed samples. Similarly, to perform such analyses under wet and dry conditions, the samples were re-suspended in 200 μL of water. Details of the reaction and characterization experimental procedures are provided in the SI.

Independent of the amount of water, no conversion of PP into chemical products was detected for the control (*i.e.* without any solid support acting as the catalyst) and blank (*i.e.* using c-HAp as the catalyst) reactions. Thus, regardless of whether the analyses were performed under immersed, wet or dry conditions, clean ^{1}H NMR spectra were obtained after 2 h under 1 sun irradiation, as is shown in Fig. 3a (complete spectra are displayed in Fig. S5). Conversely, ^{1}H NMR spectra of the water used to immerse the upp-catalyst and the PP waste allowed the identification of EtOH, with the quartet (CH_2) and the triplet (CH_3) at 3.67 and 1.20 ppm (Fig. 3a), respectively, after 2 h of irradiation. On the other hand, when the amount of available water was decreased to that used for wetting the upp-HAp catalyst, a small amount of ^{i}PrOH with the doublet and the heptuplet at 1.06 and 3.91 ppm, respectively (Fig. 3a, inset), was identified after 2 h under 1 sun irradiation. Finally, a small amount of $^{\bullet}CH_3$ radicals, with a singlet at 0.08 ppm (Fig. 3a), was identified for the reactions with upp-HAp in the dry state, which was attributed to the lack of any source for the hydroxyl group.

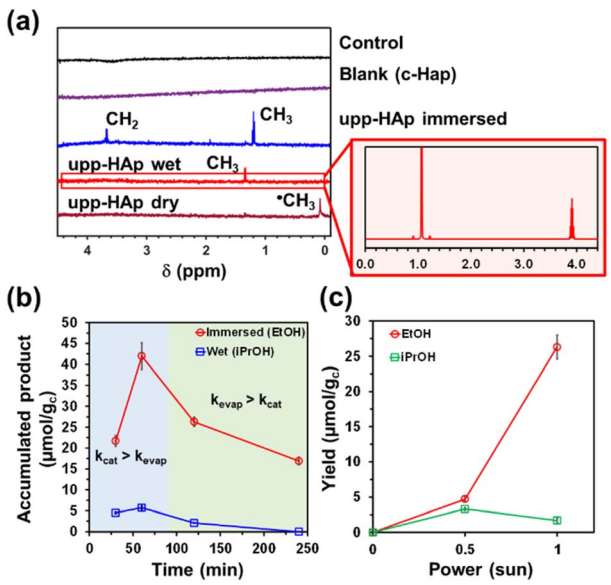

Fig. 3 (a) ^{1}H NMR spectra of the control and blank reactions and of reactions with the upp-HAp catalyst under immersed, wet and dry conditions. In all cases, reactions were conducted for 2 h under one sun irradiation. The inset shows another spectrum specifically recorded to differentiate the septuplet of isopropanol $\delta = 3.91$ ppm (–CH– group), in which the signal-to-noise ratio was increased considerably. To do so, a high-resolution measurement consisting of 64 sets of 128 scans (a total of 8192 scans) was acquired overnight. Complete spectra (including the water signal) are displayed in Fig. S3. (b) Variation of accumulated EtOH and ^{i}PrOH with time for the reaction of PP with upp-HAp under 1 sun irradiation under immersed and wet conditions, respectively. (c) Variation of the yield of EtOH and ^{i}PrOH for the reaction of PP with upp-HAp under 1 sun irradiation under immersed conditions.

The kinetics of PP MP conversion into EtOH and ^{i}PrOH using upp-HAp was followed considering the immersed and wet conditions, respectively, for reactions of up to 4 h. The recorded ^{1}H, which are displayed in Fig. S6, were used to quantify the reaction products. Fig. 3b displays the variation of the accumulated products with time. Products were quantified by calibrating the ^{1}H NMR spectra of the obtained compounds through external references, as is indicated in the SI (Fig. S7). The accumulation of products is controlled by two processes: the catalytic conversion of PP into alcohols and the evaporation of the alcohols. The conversion of PP into alcohols is the dominant process at short times, <1.5 h ($k_{cat} > k_{evap}$), while at large times, when the amount of alcohol in water increases, the vapour pressure effects (*i.e.* the vapour pressure at 25 °C of EtOH, ^{i}PrOH and water is 0.0773, 0.0579 and 0.0312 atm, respectively) favour their evaporation ($k_{evap} > k_{cat}$). The evaporation of the alcohols is supported by the increasing temperature of the system, which began to warm up after 60 min (Fig. S8). Infrared camera images acquired along 4 h showed that the temperature under 1 sun irradiation ranged increased from 22 to 27 °C after 4 h (Fig. S8). The reached temperature also allows to rule out the possible thermal degradation of PP waste, confirming the catalytic photodegradation process.

On the other hand, Fig. 3c shows the influence of illumination on the product yield and selectivity under the immersed conditions. When the power was halved, the yield of EtOH decreased by a factor of around 5.5 and the selectivity, which was 94% under 1 sun irradiation, decreased to 59%. A tentative mechanism is suggested by these features, together with the fact the yield of ^{i}PrOH decreases with increasing power irradiation. Thus, upp-HAp promotes the photodegradation of PP and the formation of $^{\bullet}CH_3$ radicals. Such radicals react among them and with hydroxyl groups from water, forming EtOH, when water is abundant enough and the energy to promote water hydrolysis is high enough (*i.e.* the formation of C–OH bonds is as favourable as the formation of C–C bonds). Instead, $^{\bullet}CH_3$ radicals tend to form a longer alkyl chain, forming ^{i}PrOH, when the OH source and the power illumination are not enough (*i.e.* the formation of C–C bonds is favoured over the formation of C–OH bonds).

The efficiency of the reaction in terms of PP mass loss corresponds to 1.6% ± 0.2% for 2 h under 1 sun irradiation. In order to improve the performance of this reaction in the future,

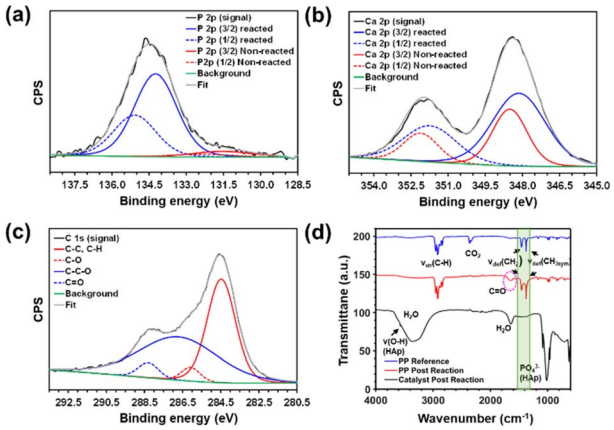

Fig. 4 (a–c) High resolution XPS spectra of (a and b) upp-HAp and (c) PP waste after the 2 h reaction under immersed conditions: (a) P 2p, (b) Ca 2p and (c) C 1s. Wide peak broadening of C–C–O has been attributed to the presence of intermediate species. (d) FTIR spectra of the same systems.

the possible mechanism of catalytic degradation has been studied using X-ray photoelectron spectroscopy (XPS). Fig. 4 displays the high resolution XPS spectra of P 2p, Ca 2p and C 1s recorded for the upp-HAp catalyst after a reaction of 2 h under immersed conditions, while the survey spectrum is displayed in Fig. S9. Comparison with the XPS spectra recorded before the reaction (Fig. S9–S11) reveals significant differences. The P2p and Ca 2p peaks of upp-HAp before the reaction can be decomposed into two peaks with a spin orbit splitting for $p_{1/2}$ and $p_{3/2}$ levels. More specifically, the decomposed peaks appear at 132.8 and 131.6 eV for P 2p (Fig. S10a), and at 351.7 and 348.1 eV for Ca 2p (Fig. S10b). Interestingly, each of the P 2p and Ca 2p peaks of the upp-HAp catalyst after the reaction are split into two (Fig. 4a and b), which is attributed to the detection of the catalyst that had not participated in the catalytic degradation of PP (peaks of lower intensity) and of the catalyst that had participated in said reaction (peaks of higher intensity).

Fig. 4a shows that, in the case of P 2p, the $p_{1/2}$ and $p_{3/2}$ peaks of the unreacted catalyst (at 132.8 and 131.6 eV, respectively) were separated by 2.3–2.6 eV from the $p_{1/2}$ and $p_{3/2}$ peaks of the reacted catalyst (at 135.1 and 134.2 eV, respectively). This significant shift clearly indicates that the destruction of hydrocarbon C–C bonds occurs at the PO_4^{3-} Lewis basic binding sites. Thus, the positive shift of the binding energies after the reaction indicates that the adsorbed species is more electronegative than P 2p, which results in a reduction of the electron density around the site. On the other hand, Fig. 4b shows that the separation between the $p_{1/2}$ and $p_{3/2}$ peaks of Ca 2p from unreacted (352.2 and 348.5 eV, respectively) and reacted (351.7 and 348.1 eV, respectively) is 0.5 eV only. This small negative shift has been associated not with the adsorption of species at the acidic Ca^{2+} binding sites but with the change in the chemical environment of the neighboring basic sites.

Two peaks appear in the C 1s XPS spectrum of pristine PP (Fig. S11). The first peak, which is located at 284.4, is directly related to the nature of the polymer (C–C and $–CH_n$ bonds), while the second peak at 286.2 is associated with C–O bonds formed by the natural aging of the polymer.[14] The appearance of new peaks at 288.3 and 286.8 eV, which are attributed to the formation of new compounds bearing C=O and C–C–O bonds, respectively, together with the decrease in the intensity of the peak at 286.2 eV, which is associated with the transformation of the species generated by natural aging, confirm the rapid catalytic degradation of PP waste (Fig. 4c). The degradation of PP is supported by the FTIR spectra of PP before and after the 2 h reaction (Fig. 4d). In addition to the differences in the bands associated with the $–CH_2–$ and CH_3 groups, a new band appears after the reaction at 1620 cm^{-1}, which has been attributed to the C=O containing formed compounds.

This work represents a proof of concept about the catalytic photodegradation of PP waste using upp-HAp and solar energy. The results allow the extension of the application of such catalytically active bioceramics, providing a potential strategy for MP remediation. The high surface of basic sites plays a key role in converting PP into EtOH or ^{i}PrOH, depending on the amount of available water. With excess water, a selectivity of 94% towards EtOH was achieved. Due to the wide distribution of MP waste, the feasibility of upp-HAp to convert this into chemicals is a simple, low-cost and promising strategy that deserves further investigation. It is worth noting that, in addition to the mild energetic conditions required (*i.e.* no temperature, pressure or electrical currents are needed) and the abundant and green nature of the catalyst used, the degradation reported presents a high selectivity towards products while avoiding potentially toxic intermediates and/or undesired residues. Future research will be focused on two key aspects of this technology: (1) enhance the efficiency of the reaction, and (2) analyse the reliability of the process using other MPs, including rubbers.

Conflicts of interest

The authors declare that the preparation of upp-HAp and its utilization for MP removal were patented: PCT/EP2023/050902 and EP25382785, respectively.

Data availability

The data supporting this article have been included as part of the supplementary information (SI). Supplementary information: methods, X-ray diffractogram, Raman and absorption spectra, complete ^{1}H NMR spectra, EIS data, infrared camera images, and XPS spectra. See DOI: https://doi.org/10.1039/d5su00734h.

Acknowledgements

This work was supported by the Fundación BBVA (WaP-HAp project). This publication is part of Maria de Maeztu Units of Excellence Programme CEX2023-001300-M, funded by MCIN/AEI/10.13039/501100011033. Support for the research of C.A. was also received through the prize "ICREA Academia" for excellence in research funded by the Generalitat de Catalunya.

Notes and references

1 (*a*) D. J. Sarkar, S. D. Sarkar, B. K. Das, J. K. Praharaj, D. K. Mahajan, B. Purokait, T. R. Mohanty, D. Mohanty, P. Gogoi and S. Kumar, *J. Hazard. Mater.*, 2021, **413**, 125347; (*b*) I. Ali, X. Tan, J. Y. Li, C. S. Peng, I. Naz, Z. P. Duan and Y. L. Ruan, *J. Clean. Prod.*, 2022, **376**, 134314.

2 N. P. Ivleva, *Chem. Rev.*, 2021, **121**, 11886.

3 (*a*) J. Martin, A. Lusher, R. C. Thompson and A. Morley, *Sci. Rep.*, 2017, **7**, 10772; (*b*) L. C. De Sá, M. Oliveira, F. Ribeiro, T. L. Rocha and M. N. Futter, *Sci. Total Environ.*, 2018, **645**, 1029; (*c*) L. Ding, R. Mao, S. Ma, X. Guo and L. Zhu, *Water Res.*, 2020, **174**, 11563.

4 (*a*) A. B. Silva, M. F. Costa and A. C. Duarte, *Curr. Opinion Environ. Sci. Health*, 2018, **1**, 30; (*b*) J. Zhang, D. Gao, Q. Li, Y. Zhao, L. Li, H. Lin, Q. Bi and Y. Zhao, *Sci. Total Environ.*, 2020, **704**, 135931.

5 S. Raju, M. Carbery, A. Kuttykattil, K. Senthirajah, A. Lundmark, Z. Rogers, S. SCB, G. Evans and T. Palanisami, *Water Res.*, 2020, **173**, 115549.

6 Z. Yang, S. Li, S. Ma, P. Liu, D. Peng, Z. Ouyang and X. Guo, *Sci. Total Environ.*, 2021, **771**, 145377.

7 (*a*) L. Wang, C. Shi, L. Pan, X. Zhang and J.-J. Zou, *Nanoscale*, 2020, **12**, 4790; (*b*) Z. Wang, T. Lin and W. Chen, *Sci. Total Environ.*, 2020, **700**, 134520; (*c*) B. Ma, W. Xue, C. Hu, H. Liu, J. Qu and L. Li, *Chem. Eng. J.*, 2019, **359**, 159; (*d*) M. Shen, T. Hu, W. Huang, B. Song, G. Zeng and Y. Zhang, *Chem. Eng. J.*, 2021, **421**, 129918; (*e*) A. Misra, C. Zambrzycki, G. Kloker, A. Kotyrba, M. H. Anjass, I. Franco Castillo, S. G. Mitchell, R. Güttel and C. Streb, *Angew. Chem., Int. Ed.*, 2020, **59**, 1601.

8 (*a*) M. Du, Y. Zahng, S. Kang, X. Guo, Y. Ma, M. Xing, Y. Zhu, Y. Chai and B. Qiu, *ACS Catal.*, 2022, **12**, 12823; (*b*) Y. Miao, Y. Zhao, J. Gao, J. Wang and T. Zhang, *J. Am. Chem. Soc.*, 2024, **146**, 4842; (*c*) S. Zhang, H. Li, L. Wang, J. Liu, G. Liang, K. Davey, J. Ran and S. Z. Qiao, *J. Am. Chem. Soc.*, 2023, **145**, 6410; (*d*) A. Sun and W. X. Wang, *Environ. Sci. Technol.*, 2023, **57**, 8118; (*e*) J. Qin, Y. Dou, J. Zhou, V. M. Candelario, H. R. Andersen, C. Helix-Nielsen and W. Zhang, *Adv. Funct. Mater.*, 2023, **33**, 2214839; (*f*) C. X. Liu, K. Liu, Y. Xu, Z. Wang, Y. Weng, F. Liu and Y. Chen, *Angew. Chem., Int. Ed.*, 2024, **63**, e202401255.

9 (*a*) U. Anand, S. Dey, E. Bontempi, S. Ducoli, A. D. Vethaak, A. Dey and S. Federici, *Environ. Chem. Lett.*, 2023, **21**, 1787; (*b*) P. Ebrahimbabaie, K. Yousefi and J. Pichtel, *Sci. Total Environ.*, 2022, **806**, 150603.

10 (*a*) J. Sans, M. Arnau, V. Sanz, P. Turon and C. Alemán, *Chem. Eng. J.*, 2022, **433**, 1335512; (*b*) J. Sans, G. Revilla-López, V. Sanz, J. Puiggalí, P. Turon and C. Alemán, *Chem. Commun.*, 2021, **57**, 5163; (*c*) J. Sans, M. Arnau, V. Sanz, P. Turon and C. Alemán, *Chem. Eng. J.*, 2022, **446**, 137440; (*d*) J. Sans, M. Arnau, R. Bosque, P. Turon and C. Alemán, *Sustainable Energy Fuels*, 2024, **8**, 1473.

11 (*a*) J. Sans, M. Arnau, P. Turon and C. Alemán, *Mater. Horizons*, 2022, **9**, 1566; (*b*) J. Sans, M. Arnau, A. Fontana-Escartín, P. Turon and C. Alemán, *Chem. Mater.*, 2023, **35**, 3765; (*c*) J. Sans, M. Arnau, J. J. Roa, P. Turon and C. Alemán, *ACS Appl. Nano Mater.*, 2022, **5**, 8526.

12 J. Sans, M. Arnau, V. Sanz, P. Turon and C. Alemán, *Chem. Eng. J.*, 2022, **433**, 133512.

13 P. Makuła, M. Pacia and W. Macyk, How to correctly determine the band gap energy of modified semiconductor photocatalysts based on UV-Vis spectra, *J. Phys. Chem. Lett.*, 2018, **9**, 6814.

14 (*a*) K. Yamamoto, H. Asahara, K. Harada, Y. Itabashi, K. Ohkubo and T. Inoue, *J. Mater. Chem. B*, 2023, **11**, 5101; (*b*) A. Rjeb, S. Letarte, L. Tajounte, M. C. El Idrissi, A. Adnot, D. Roy, Y. Claire and J. Kaloustian, *J. Electron Spectrosc. Relat. Phenom.*, 2000, **107**, 221.